Received June 11, 2018, accepted July 2, 2018, date of publication July 5, 2018, date of current version July 30, 2018.

Digital Object Identifier 10.1109/ACCESS.2018.2853140

Delay-Universal Channel Coding With Feedback

MD. NOOR-A-RAHIM[1], M. O. KHYAM[2], YONG LIANG GUAN[1], G. G. MD. NAWAZ ALI[3], KHOA D. NGUYEN[4], AND GOTTFRIED LECHNER[4]

[1]School of Electrical and Electronic Engineering, Nanyang Technological University, Singapore 639798
[2]Department of Mechanical Engineering, Virginia Tech, Blacksburg, VA 24061, USA
[3]Department of Automotive Engineering, Clemson University, Clemson, SC 29634, USA
[4]Institute for Telecommunications Research, University of South Australia, Adelaide, SA 5001, Australia

Corresponding author: Md. Noor-A-Rahim (narahim@ntu.edu.sg)

This work was supported by the NTU-NXP Intelligent Transport System Test-Bed Living Lab Fund through the Economic Development Board, Singapore, under Grant S15-1105-RF-LLF.

ABSTRACT In this paper, the design of error-correcting or channel codes for delay-universal/anytime communication is shown while considering systems with and without a feedback link. We construct practical and low complexity anytime channel codes based on spatially-coupled repeat-accumulate (SC-RA) codes. Performance and density evolution analysis are shown for the binary erasure channel (BEC) and the binary input additive white Gaussian noise (BIAWGN) channel. We observe that the erasure/error floors exist even at low decoding delay in the following cases: 1) when the code rate is close to the Shannon capacity; and/or 2) when the code parameters are chosen to target a high decaying rate of erasure/error probability. To mitigate erasure/error floors, we present feedback algorithms for BEC and BIAWGN channels. We show that the proposed feedback strategies can greatly enhance the performance of anytime SC-RA codes. Numerical results also show that the feedback strategies significantly reduce the decoder complexity. The proposed feedback approach is applied to an aircraft tracking application to track/calculate/estimate the state information of the aircraft. Based on comparisons of the results obtained from the traditional block and anytime coding scenarios, it is observed that the latter significantly outperforms the former in terms of tracking performance.

INDEX TERMS Delay-universal/anytime communication, feedback, estimation, reliability.

I. INTRODUCTION

In control applications, the controller needs to track system state information over a noisy channel. For timely and appropriate control actions, reliable real-time system state information is required at the controller. In other words, both transmission reliability and delay are important in control applications. However, classical communication techniques, which utilize block or convolutional codes, are not suitable for this purpose, because they trade off delay for reliability. For example, traditional block codes attain reliability only at infinite delays which results in instability in closed loop controls [1]. In contrast, delay-universal or anytime communication [2] was shown to be necessary and sufficient for tracking and controlling unstable plants over a noisy channel. In anytime communication, the *delay-exponent* is an important performance measure, which specifies how fast the error probability decays with the delay.

In recent years, the design of practical error-correcting or channel codes for anytime communication has been studied in [3]–[7]. These channel codes are often known as anytime codes. Anytime codes with fixed structure are studied in [3]–[5], while anytime codes with random structure are studied in [6]. In this paper, we focus on random structured anytime codes. The random structured anytime codes, presented in [6], can avoid error floors up to a significant level provided that the memory length is very large and the delay-exponent is low. However, a code with very large memory raises the computational complexity at both encoder and decoder. On the other hand, high speed decaying of error probability is highly desirable in practical systems. Thus, in practice, a code with moderate memory length is required which can provide high delay exponents. These requirements are not attainable with the existing random structured anytime framework. Moreover, the anytime codes of [6] suffer from high encoding complexity.

In this work, we present a practical anytime coding scheme based on spatially coupled repeat-accumulate (SC-RA) codes and investigate the anytime performance over the binary erasure channel (BEC) and the binary input additive white Gaussian noise (BIAWGN) channel.[1] For both channels, an asymptotic analysis of the proposed anytime coding scheme is presented by deriving corresponding *density evolution* recursions. The performance of the proposed codes is compared with existing anytime codes and numerical results are presented for different scenarios. From the comparison, we show that SC-RA anytime codes outperform the anytime codes presented in [6], while offering simpler encoding implementations. We also observe that high erasure/error floors appear at the performance of the anytime code when the memory length is limited and/or the delay-exponent is high. To mitigate this problem, we present feedback algorithms for both channels and show that the feedback schemes significantly improve the performance of anytime SC-RA codes.[2] Furthermore, the proposed feedback strategies reduce the complexity of the anytime decoder. We also apply the proposed scheme in tracking the system state information of an aircraft and show the effectiveness of the proposed scheme over traditional schemes.

The rest of the paper is organized as follows. In Section II, we describe anytime communication and SC-RA code. In Section III, the design of the anytime coding scheme based on SC-RA codes is shown and density evolution analysis is presented over BEC and BIAWGN channels. In this section, we also show the performance comparison with existing anytime codes and present the asymptotic and finite-length results for different scenarios. The feedback algorithms for BEC and BIAWGN channels are presented in IV. In Section V, we show an example of practical application, where the effectiveness of the proposed scheme is shown. Finally, concluding summaries are drawn in Section VI.

II. BACKGROUND

A. ANYTIME CHANNEL CODE

Let a streaming source produce a K-bit message $\boldsymbol{m}_t \in \{0, 1\}^K$ each time instant t. An anytime channel encoder takes all the produced messages up to time instant t and produces a M-bit encoded message $\boldsymbol{x}_t \in \{0, 1\}^M$ with a code rate $R_c = \frac{K}{M}$. Mathematically, the function of the anytime channel encoder can be defined by $\boldsymbol{x}_t = \mathcal{E}_t(\boldsymbol{m}_1^t)$, where $\boldsymbol{m}_1^t = [\boldsymbol{m}_1, \boldsymbol{m}_2, \ldots, \boldsymbol{m}_t]$. The encoded message $\boldsymbol{x}_t$ is then transmitted over a noisy channel and the receiver obtains $\boldsymbol{y}_t$ (a noisy version of $\boldsymbol{x}_t$). The anytime channel decoder estimates the current as well as all previous messages based on all the received messages. At time instant t, let $\hat{\boldsymbol{x}}_i(t)$ be the estimated message corresponding to message $\boldsymbol{x}_i$. The decoding function can be written as $\hat{\boldsymbol{x}}_1^t(t) = \mathcal{D}_t(\boldsymbol{y}_1^t)$, where $\hat{\boldsymbol{x}}_1^t(t) = [\hat{\boldsymbol{x}}_1(t), \hat{\boldsymbol{x}}_2(t), \ldots, \hat{\boldsymbol{x}}_t(t)]$ and $\boldsymbol{y}_1^t = [\boldsymbol{y}_1, \boldsymbol{y}_2, \ldots, \boldsymbol{y}_t]$. A block diagram of anytime communication is illustrated in Fig. 1.

[1]Part of this paper was presented in [7], where the code construction of SC-RA anytime codes was shown.

[2]Note that many previous works, such as [8]–[11], have performed theoretical investigations on the benefits of feedback links in anytime communication. However, very limited works have investigated the impact of feedback links on the performance of practical anytime codes.

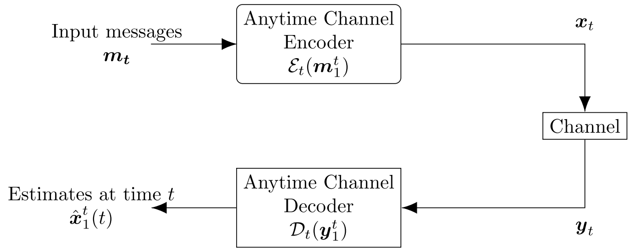

FIGURE 1. A block diagram illustrating anytime communication.

For an estimated message $\hat{\boldsymbol{x}}_i(t)$ the corresponding decoding delay is $d = t - i$. The error probability of message $\boldsymbol{x}_i$ at decoding delay d can be written as $\mathbb{P}_e(i, d) = \Pr\big(\hat{\boldsymbol{x}}_i(i + d) \neq \boldsymbol{x}_i\big)$. For a given channel, the encoder-decoder pair $(\mathcal{E}_t, \mathcal{D}_t)$ is called *anytime* or *delay-universal* code if there exists $\alpha, \beta > 0$ such that [12]:

$$\mathbb{P}_e(i, d) \leq \beta e^{-\alpha d}, \quad \forall d \geq 0, \tag{1}$$

where β is a constant and $\alpha > 0$ is known as the *anytime reliability* or *delay-exponent* [1]. The delay-exponent α specifies how fast the reliability of the system improves with delay. The inequality in (1) is the major property of an anytime decoder. (1) implies that at any delay $d \geq 0$, the decoder is able to estimate the message $\boldsymbol{x}_i$ and the probability of error for that message will exponentially decay to zero when the delay d approaches infinity.

B. SPATIALLY COUPLED RA CODES

Spatially coupled codes based on LDPC codes were first analytically investigated in [13]. Later, spatially coupled RA codes were introduced in [14]. SC-RA codes are constructed from RA protographs. A RA protograph represents a small RA code, which consists of two types of variable nodes (namely information bit nodes and parity bit nodes) and one type of check nodes. In a (Q, A)-regular RA code, every information bit node is connected to exactly Q check nodes and every check node is connected to exactly A information bit nodes. A SC-RA code can be realized in two steps: (i) firstly by coupling a chain of L standard (Q, A)-regular RA protographs such that each of the Q connections of a message bit node at position i is uniformly connected to their neighboring check nodes in the range $i - (\gamma - 1)/2$ to $i + (\gamma - 1)/2$ (ii) then by lifting and connecting the coupled protograph similar to the lifting and connecting done for protograph-based LDPC codes [15]. We consider L as the chain length, γ as the coupling length and M as the lifting factor. Thus, each protograph/position contains M message bit nodes, $\frac{Q}{A}M$ check nodes and $\frac{Q}{A}M$ parity bit nodes. A terminated coupled protograph can be achieved by adding extra check nodes and parity bit nodes on both sides of the chain. Fig. 2 shows a coupled protograph of a SC-RA code. The design rate of the

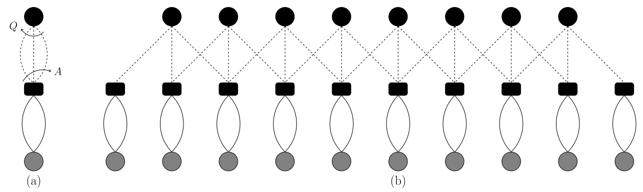

FIGURE 2. **(a) A RA protograph, where the dark circle node represents message bit nodes, the gray circle node represents parity bit nodes, and the dark rectangular node represents check nodes. (b) Spatially coupled RA code created from a chain of regular $(Q, A) = (3, 3)$ protographs, where $L = 8$ and $\gamma = 3$.**

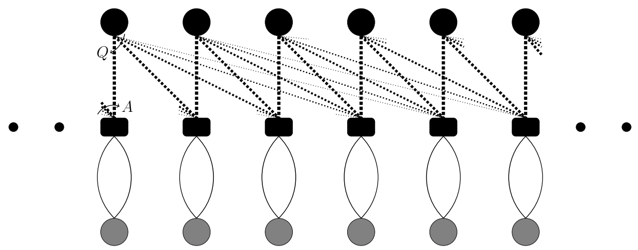

FIGURE 3. **Tanner graph of anytime spatially coupled RA code. In the figure, the dotted lines represent the probabilistic edge connections. The exponential distribution of the edges is depicted through the variation in the thickness of the dotted lines.**

spatially coupled RA code is given by [14]:

$$R_d(Q, A, \gamma, L) = \frac{L}{L + \frac{Q}{A}\Big\{L - \gamma + 1 + 2\big(\gamma - \sum_{i=0}^{\gamma}(\frac{i}{\gamma})^A\big)\Big\}}. \tag{2}$$

Asymptotically the code rate becomes

$$\lim_{\gamma\to\infty}\lim_{L\to\infty} R_d(Q, A, \gamma, L) = \frac{A}{A+Q}. \tag{3}$$

In [14], it was shown that SC-RA codes exhibit better decoding thresholds than SC-LDPC codes, while SC-RA codes have simple encoding property. These features make SC-RA codes more suitable than SC-LDPC codes in linear anytime code designs.

C. DECODING ALGORITHMS

For the decoding of anytime code, we consider message passing algorithm with expanding window decoding technique [3]. When a new message of the anytime code sequence arrives at time instance t, the decoder performs message-passing on the entire sequence of received messages from time instance 1 to t. In the next time step, the decoding window is expanded to include the next code block. The operational structure of the expanding window decoding technique is shown schematically in Fig. 4. The following message passing decoding algorithms are considered in this paper.

1) ERASURE DECODING

Over BEC, a transmitted bit is either received correctly or completely unknown. In the conventional decoder

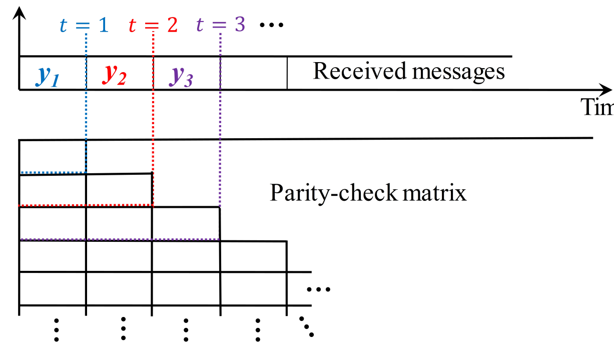

FIGURE 4. **Expanding window decoding of anytime code.**

for BEC, message passing between variable node and check node occurs in the following manner. At each iteration, a variable node V whose value is known (either from the channel output or from previous iterations) sends its value to the connected check nodes, and a variable node whose value is not yet known/recovered sends an erasure symbol. On the other hand, a check node C sends to a connected variable node V an erasure if it receives at least one erasure from the connected variable nodes other than V; otherwise C sends to V the sum (mod 2) of all incoming messages except the message from V. Note that an extended version of erasure decoding called peeling decoding [16] is considered in this paper, where the decoding window size depends only on the number of erased bits. Since the decoder can accurately detect the recovered bits for the BEC, the erasure performance of the peeling decoder remains the same as for the conventional decoder. In the peeling decoding algorithm, at each decoding time instant, the decoder first removes the recovered (non-erased) coded bits and the corresponding columns of parity check matrix. Then the all-zero rows of the check matrix are removed. These steps result in a reduced check matrix size, over which the erasure decoding algorithm is performed.

2) BELIEF PROPAGATION DECODING

For BIAWGN channels, Belief Propagation (BP) decoding algorithm is the most prominent category of message passing algorithms. In the belief propagation algorithm, the messages are expressed as Log likelihood ratios (LLRs) to simplify the mathematical operations. Let x_i and y_i be the channel input and output corresponding to the variable node i. The LLR obtained from the channel for variable node i is defined by

$$r_i = \log\frac{P_{\mathrm{ch}}(y_i|x_i = 0)}{P_{\mathrm{ch}}(y_i|x_i = 1)}, \tag{4}$$

where $P_{\mathrm{ch}}(\cdot)$ represents channel transition probability. At the beginning of the BP decoding process, each variable node sends the corresponding LLR obtained from the channel to the connected check nodes. Let $\mathbb{S}_v(i)$ represent the set of variable nodes that are connected with the i^{th} check node. Similarly, let $\mathbb{S}_c(i)$ represent the set of check nodes that are connected with the i^{th} variable node. Let $F_{j,i}^{(\ell)}$ be the message sent from variable node i to check node j at iteration ℓ.

The message sent from check node j to variable node i at iteration ℓ is [17, Ch. 2]:

$$G_{j,i}^{(\ell)} = 2\tanh^{-1}\left(\prod_{i' \in \mathbb{S}_v(j), i' \neq i} \tanh\left(\frac{F_{j,i'}^{(\ell)}}{2}\right)\right). \quad (5)$$

Based on the messages from check nodes, the message sent from a variable node i to check node j is

$$F_{j,i}^{(\ell+1)} = \sum_{j' \in \mathbb{S}_c(i), j' \neq j} G_{j',i}^{(\ell)} + r_i. \quad (6)$$

For a fixed number of iterations, the complexity of the above message passing decoders scales linearly with the number of edges. Since the number of edges grows linearly with the increasing of decoding window length, the complexity of the above decoders scales linearly with the number of messages received by the decoder. In other words, the decoding complexity (specially for BP decoding) grows linearly with the decoding delay.

III. ANYTIME CODES BASED ON SPATIALLY COUPLED RA CODES

A. CODE DESIGN

Similar to [6], we modify the structure of spatially coupled RA codes in the following manner to achieve the anytime coding properties:

1) To ensure causal streaming and anytime decoding capability, each of the Q connections of a message bit node at position i is independently chosen from the check nodes in the range of $[i, ..., i + \gamma - 1]$.
2) Instead of a uniform distribution of each connection from message bit nodes to check nodes, we choose an exponential distribution so that a message bit node at position i has more connections with the check nodes closer to position i. This type of distribution allows a quick improvement of the error performance with small delay. With an exponential distribution, the probability of a connection between a message bit node at position i and a check node at position j ($j \geq i$) can be written by:

$$\Pr(k) = \frac{e^{-k\lambda}(1 - e^{-\lambda})}{1 - e^{-\gamma\lambda}}, \quad (7)$$

where λ is known as exponential rate parameter and $k = j - i$ is the distance between the connected check node and message bit node. For $\gamma = \infty$, (7) becomes

$$\Pr(k) = e^{-k\lambda}(1 - e^{-\lambda}). \quad (8)$$

On the other hand, the degree of the parity bit nodes is two and a parity node at position i is only connected to the check node at position i. In this paper, we refer to the above mentioned code as (Q, A, λ, γ)-anytime SC-RA code.

A realized protograph of the (Q, A, λ, γ)-anytime SC-RA code with the above structure is shown in Fig. 3. In the rest of the paper, we represent all the variable nodes at position i (i.e., combination of message bit and parity bit nodes at position i) as the encoded message $\boldsymbol{x}_i$. In the following section, we present the performance analysis of (Q, A, λ, γ)-anytime SC-RA codes over BEC and BIAWGN channels.

Remarks on the Difference Between Conventional SC-RA Code and the Proposed Anytime SC-RA Code: The conventional SC-RA code [14] considers very limited γ (usually $\gamma = Q$), which results in a convolutional code with finite memory length and thus the error performance levels out with increasing delay. The results in Fig. 5 illustrate this phenomenon, where the conventional SC-RA code is shown to have worse performance than our proposed anytime code (with large γ). Furthermore, the uniform distribution used in the conventional SC-RA code cannot ensure a quick recovery of recently received messages (which is a desired property of a anytime code). The use of exponential distribution in our proposed code enables this desired property.

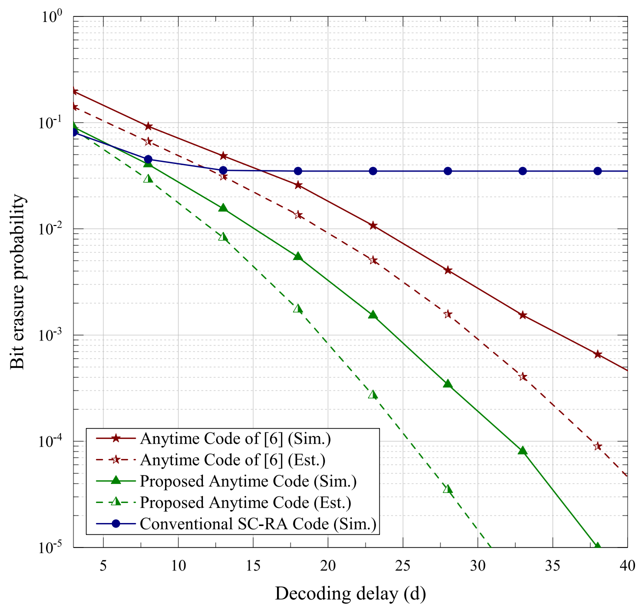

FIGURE 5. Performance comparison between SC-LDPC anytime codes [6] and our proposed SC-RA anytime code. Simulation and estimation results are shown for both codes over the BEC with $\epsilon = 0.4$. Performance of the conventional SC-RA code is also plotted in the figure.

B. BEC

For the density evolution over the BEC, we denote $V_m^{(\ell)}(i,t)$ and $V_p^{(\ell)}(i,t)$ as the erasure probabilities from information bits and parity bits, respectively, of message $\boldsymbol{x}_i$, at iteration ℓ when $t \geq i$ messages are received. The density evolution equations of anytime spatially coupled RA codes over the BEC are given in (9) and (10), as shown at the top of the next page. We initialize the density evolution recursion by $V_m^{(\ell)}(i,t) = V_p^{(\ell)}(i,t) = 0, \forall \ell$ when $i \leq 0$ and $V_m^{(0)}(i,t) = V_p^{(0)}(i,t) = \epsilon$ when $0 < i \leq t$, where ϵ is the channel erasure probability. The probability that the information bit of message $\boldsymbol{x}_i$ has been erased can be computed after a maximum number of iteration $\ell_{\max}$ while considering the erasure

$$V_m^{(\ell+1)}(i,t) = \epsilon\left[1-\sum_{j=0}^{\infty}P_r(j)\left\{\left(1-V_p^{(\ell)}(i+j,t)\right)^2\left(1-\sum_{k=0}^{\infty}P_r(k)V_m^{(\ell)}(i+j-k,t)\right)^{A-1}\right\}\right]^{Q-1}, \quad (9)$$

$$V_p^{(\ell+1)}(i,t) = \epsilon\left[1-\sum_{j=0}^{\infty}P_r(j)\left\{\left(1-V_p^{(\ell)}(i+j,t)\right)\left(1-\sum_{k=0}^{\infty}P_r(k)V_m^{(\ell)}(i+j-k,t)\right)^{A}\right\}\right], \quad (10)$$

$$\mathbb{P}_{\text{iBEC}}(i,t) = \epsilon\left[1-\sum_{j=0}^{\infty}P_r(j)\left\{\left(1-V_p^{(\ell_{\max})}(i+j,t)\right)^2\left(1-\sum_{k=0}^{\infty}P_r(k)V_m^{(\ell_{\max})}(i+j-k,t)\right)^{A-1}\right\}\right]^{Q}. \quad (11)$$

$$V_m^{(\ell+1)}(i,t) = \frac{2}{\sigma_n^2} + (Q-1)\mathcal{J}^{-1}\left[\sum_{j=0}^{\infty}\Pr(j)\mathcal{J}\left\{\phi^{-1}\left(1-\left\{1-\phi\left(V_p^{(\ell)}(i+j,t)\right)\right\}^2\right.\right.\right.$$
$$\left.\left.\left.\times\left\{1-\phi\left(\mathcal{J}^{-1}\left(\sum_{k=0}^{\infty}\Pr(k)\mathcal{J}\left(V_m^{(\ell)}(i+j-k,t)\right)\right)\right)\right\}^{A-1}\right)\right\}\right], \quad (13)$$

$$V_p^{(\ell+1)}(i,t) = \frac{2}{\sigma_n^2} + \mathcal{J}^{-1}\left[\sum_{j=0}^{\infty}\Pr(j)\mathcal{J}\left\{\phi^{-1}\left(1-\left\{1-\phi\left(V_p^{(\ell)}(i+j,t)\right)\right\}\right.\right.\right.$$
$$\left.\left.\left.\times\left\{1-\phi\left(\mathcal{J}^{-1}\left(\sum_{k=0}^{\infty}\Pr(k)\mathcal{J}\left(V_m^{(\ell)}(i+j-k,t)\right)\right)\right)\right\}^{A}\right)\right\}\right], \quad (14)$$

$$f\left(\sigma_n^2, V_i^{(\ell_{\max})}, V_p^{(\ell_{\max})}, Q, A\right) = \frac{2}{\sigma_n^2} + Q\mathcal{J}^{-1}\left[\sum_{j=0}^{\infty}\Pr(j)\mathcal{J}\left\{\phi^{-1}\left(1-\left\{1-\phi\left(V_p^{(\ell_{\max})}(i+j,t)\right)\right\}^2\right.\right.\right.$$
$$\left.\left.\left.\times\left\{1-\phi\left(\mathcal{J}^{-1}\left(\sum_{k=0}^{\infty}\Pr(k)\mathcal{J}\left(V_m^{(\ell_{\max})}(i+j-k,t)\right)\right)\right)\right\}^{A-1}\right)\right\}\right]. \quad (15)$$

probabilities of all of its connected edges. The bit erasure probability ($\mathbb{P}_{\text{iBEC}}(i,t)$) of the information bit of message $\boldsymbol{x}_i$ is given in (11), as shown at the top of this page.

C. BIAWGN CHANNEL

For the density evolution over the BIAWGN channel, we denote $V_m^{(\ell)}(i,t)$ and $V_p^{(\ell)}(i,t)$ as the mean values of LLR messages outgoing from information bit node and parity bit node, respectively at position i in the ℓ^{th} iteration when t messages are received. Following [18], the density evolution update equations over the BIAWGN channel are given in the top of this page (see (13) and (14)). In these equations, the following functions are used:

$$\phi(g) = \begin{cases} 1 - \dfrac{1}{\sqrt{4\pi g}}\displaystyle\int_{-\infty}^{\infty}\left(\tanh\frac{f}{2}\right)e^{-\frac{(f-g)^2}{4g}}df, & \text{if } g > 0 \\ 1, & \text{if } g = 0 \end{cases}$$

and

$$\mathcal{J}(g) = 1 - \frac{1}{\sqrt{4\pi g}}\int_{-\infty}^{\infty}e^{-\frac{(f-g)^2}{4g}}\log_2(1+e^{-f})df.$$

We initialize the density evolution recursions by $V_m^{(\ell)}(i,t) = V_p^{(\ell)}(i,t) = \infty, \forall\ell$ when $i \leq 0$ and $V_m^{(0)}(i,t) = V_p^{(0)}(i,t) = \frac{2}{\sigma_n^2}$ when $0 < i \leq t$, where σ_n^2 is the noise variance of the BIAWGN channel. The bit error rate ($\mathbb{P}_{\text{iAWGN}}(i,t)$) of the information bit of message $\boldsymbol{x}_i$ is given by [6],

$$\mathbb{P}_{\text{iAWGN}}(i,t) = \mathcal{Q}\left(\sqrt{\frac{1}{2}f\left(\sigma_n^2, V_i^{(\ell_{\max})}, V_p^{(\ell_{\max})}, Q, A\right)}\right), \quad (12)$$

where $f\left(\sigma_n^2, V_i^{(\ell_{\max})}, V_p^{(\ell_{\max})}, Q, A\right)$ is defined in (15), as shown at the top of this page, and $\mathcal{Q}(\cdot)$ is the Q-function defined by

$$\mathcal{Q}(x) = \frac{1}{2\pi}\int_{x}^{\infty}\exp\left(-\frac{u^2}{2}\right)du.$$

D. NUMERICAL RESULTS

In this subsection, we present the performance comparison and numerical results for the proposed SC-RA anytime codes. In the simulation, erasure decoding was considered for BEC, while BP decoding was considered for BIAWGN channel with maximum iteration of 200.[3] In Fig. 5, we show

[3]Throughout the paper, the maximum iteration for the decoders is fixed to 200.

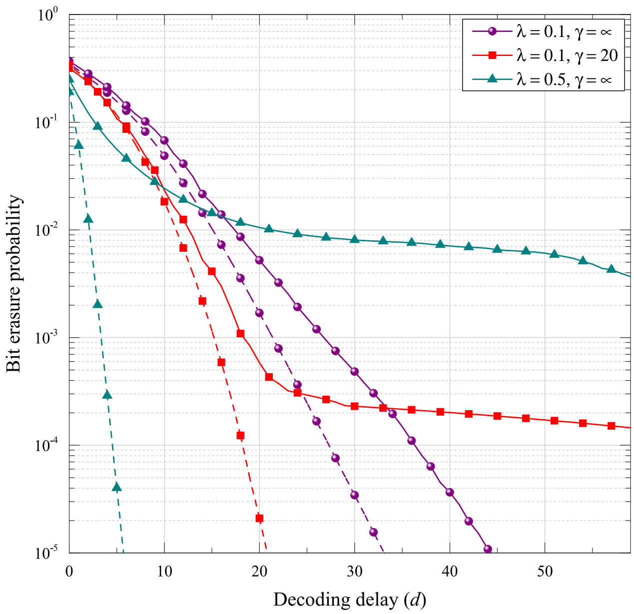

FIGURE 6. Performance of SC-RA anytime code over BEC ($\epsilon = 0.42$) while varying the design parameters. Solid lines present finite-length ($M = 16$) results, while dotted lines represent the results from density evolution.

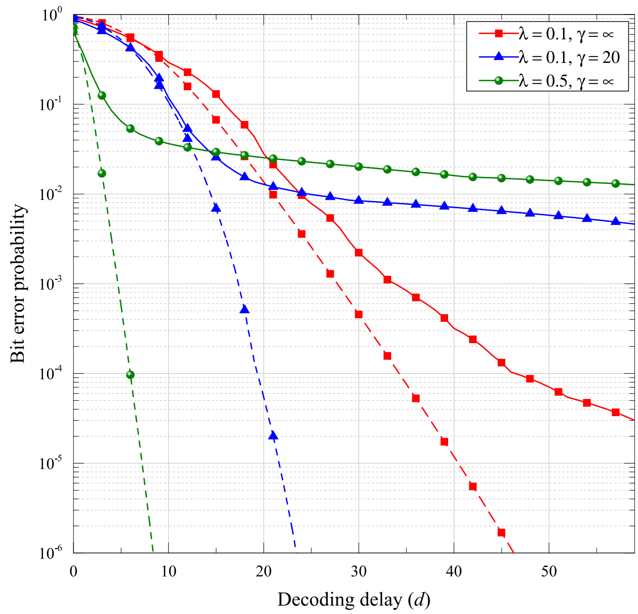

FIGURE 7. Performance of SC-RA anytime codes over the BIAWGN channel (SNR = 0.5 dB) while varying the design parameters. Solid lines present finite-length ($M = 16$) results, while dotted lines represent the results from density evolution.

the performance comparison between anytime code of [6] (based on SC-LDPC codes) and our proposed SC-RA anytime code. For the anytime SC-LDPC codes [6], we consider $(d_v, d_c) = (3, 6)$ and for the proposed SC-RA codes, we consider $(Q, A) = (4, 4)$. The code parameters are chosen such that both codes maintain an average variable and check nodes degree of 3 and 6, respectively. Thus, for both cases, the code rate is $R_d = \frac{1}{2}$. In the simulation, we consider a message size $M = 40$, $\lambda = 0.1$, $\gamma = \infty$, and $\epsilon = 0.4$ for both codes. We plot the average erasure performance of 5^{th} encoded message ($\boldsymbol{x}_5$) versus the decoding delay. At any decoding time instant t, the decoding delay (d) for $\boldsymbol{x}_5$ is calculated by $d = t-5$. Each point of the simulation results is obtained by averaging over 10^6 simulation runs. Along with the simulation results, we also show the estimation results obtained from the estimation technique of [6] to predict the finite-length performance of anytime codes. We observe that the anytime SC-RA codes provide better performance than the anytime SC-LDPC codes. In Fig. 5, we also plot the simulation performance of conventional SC-RA code with $(Q, A) = (4, 4)$, and we notice a very high error floor for this scenario. Note that we also observed above performance characteristics for the BIAWGN channel.

In Fig. 6 and Fig. 7, the performance of the anytime codes are presented for the BEC and the BIAWGN channel, respectively for different scenarios. For both cases, we present the asymptotic and finite-length results with three different scenarios. We vary the parameters λ and γ, while fixing $Q = 4$ and $A = 4$. The channel parameters considered for the BEC and the BIAWGN channel are $\epsilon = 0.42$ and signal-to-noise ratio (SNR) = 0.5 dB, respectively. For both channels, it is observed that the performance curve does not show error floors at bit erasure/error rate above 10^{-5} when the coupling length is sufficiently large and the exponential rate parameter is low. For limited coupling length and/or high exponential rate parameter, the performance curve possess a very high erasure/error floor. This is due to the fact that both limited coupling length and high exponential rate parameter result in limited memory of the code. Moreover, the connections between variable nodes and check nodes become concentrated, which creates short cycles in the resultant code. However, in the practical cases, limited coupling length and/or high exponential rate parameter are desirable. To mitigate erasure/error floor problems in such scenarios, we present feedback algorithms in the following section for the BEC and the BIAWGN channel.

IV. ANYTIME TRANSMISSION WITH FEEDBACK

We now present feedback strategies for the BEC and the BIAWGN channel to tackle the erasure/error floors in the performance of the anytime codes. We assume that the feedback link is noiseless with zero delay,[4] i.e., the information sent through the feedback link is correctly received by the encoder.

A. BEC

For the BEC, we present a threshold (in terms of decoding delay) based feedback strategy. At every time instant, the decoder looks for erasure bits in the messages whose decoding delays have exceeded a predefined threshold. If any

[4]This assumption is often considered in automatic repeat request (ARQ) transmission.

such erasure is found, the decoder activates the feedback link before the next message transmission and sends the index of the earliest erased bit through the feedback link. The encoder simply appends the requested bit value to the next coded message. If the re-transmitted bit is received successfully, the decoder may be able to recover part or all of the subsequent erased bits. Thus, with this retransmission strategy, one can improve the performance of the message where the requested bit belongs as well as the subsequent messages. Note that a similar re-transmission strategy is presented in [3], where the threshold is defined in terms of erasure-pattern set size (depends on the number of overall erasure bits at the decoder). On the other hand, the threshold in our proposed strategy is defined in terms of the decoding delay. With this proposed strategy, received messages get sufficient time to be decoded at the receiver before the activation of the feedback link. The details of this feedback strategy are provided in Algorithm 1.

Algorithm 1 Anytime Transmission With Feedback Over the BEC

- Set a threshold W_{th}.
- When $t - W_{th} > 0$:
  - The anytime encoder does the following.
    - If no retransmission request is received, the encoder maintains it's usual transmission and transmits message $\boldsymbol{x}_{t+1}$.
    - If retransmission request of a particular bit is received, the requested bit is simply transmitted along with the message $\boldsymbol{x}_{t+1}$.
  - The anytime decoder does the following.
    - Search for erased bits in the messages from $\hat{\boldsymbol{x}}_1(t)$ to $\hat{\boldsymbol{x}}_{t-W_{th}}(t)$.
    - If erasure bit is detected, then it sends the index of the earliest erasure bit via the feedback link.
    - If no erasure is found, the decoder does not activate the feedback link.

The performance improvement due to the feedback strategy is shown in Fig. 8. In the simulation, we consider $(Q, A, \lambda, \gamma) = (4, 4, 0.2, 20)$ with $\epsilon = 0.42$. We set the feedback threshold as $W_{th} = 20$. Thus the feedback link can only be activated at or after decoding time $t = 21$. The decoder performs the erasure decoding operation (as described in Subsection II-C) after placing the retransmitted bit value (in case of successful reception of the retransmitted bit) in the position of the earliest erasure bit. In Fig. 8, we present the erasure probability performance of five messages. Without feedback, the erasure probability of all the messages approaches an erasure floor. With the feedback strategy, the erasure probability performance maintains exponential decay with the decoding delay. We observe that the performance of each message is a shifted version of another. We also observe that the performance improvement of different messages is observed from decoding time $t = 20$,

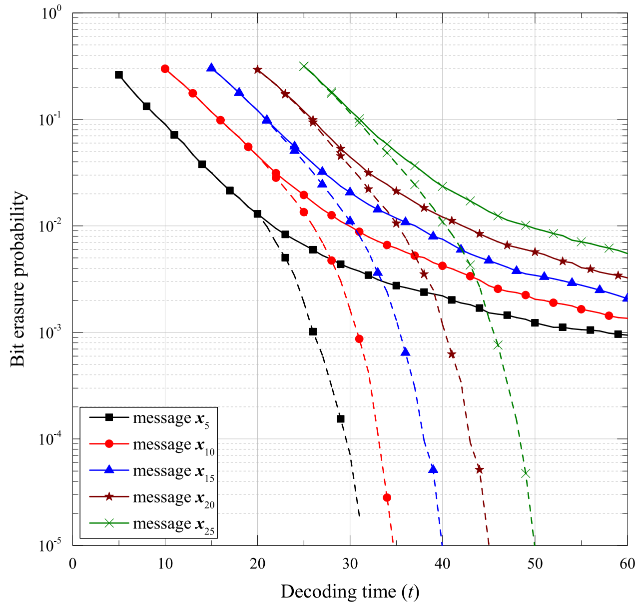

FIGURE 8. Erasure probability performance of different messages with and without feedback. Solid lines present no feedback scenario, while dotted lines represent with feedback scenario.

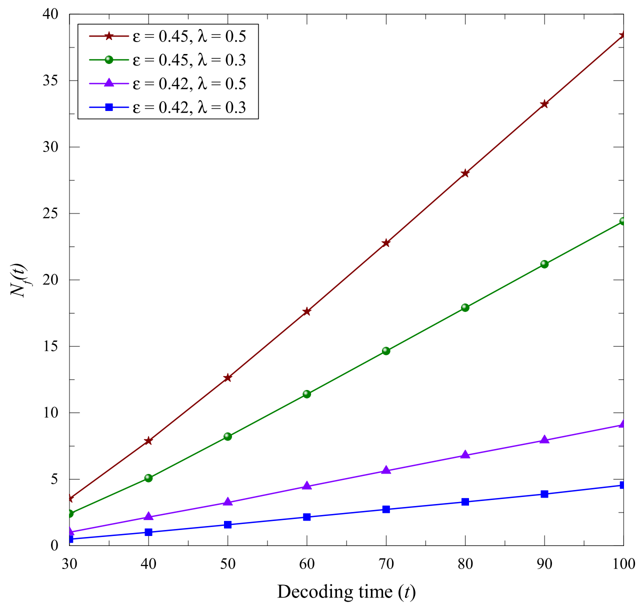

FIGURE 9. Impact of channel erasure probability (ϵ) and exponential rate parameter (λ) on the accumulated number of retransmission request $N_f(t)$.

even though their own bits are not re-transmitted. Due to the dependence of one message to another, a retransmitted bit of a previous message can improve the performance of the subsequent messages. For the above scenario, the number of feedback requests made by the decoder is close to 2 at decoding time instant 60. Let $N_f(t)$ be the accumulated number of retransmission request up to time t. In Fig. 9, we show the characteristics of accumulated number of retransmission

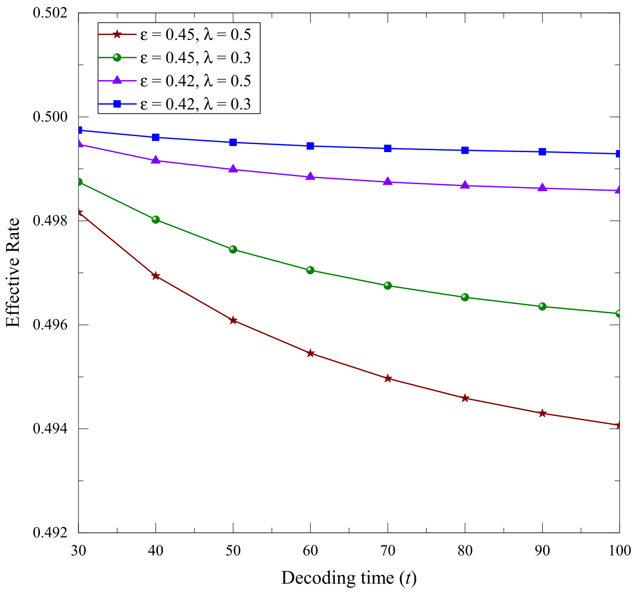

FIGURE 10. Impact of channel erasure probability (ϵ) and exponential rate parameter (λ) on the effective rate of the SC-RA anytime code.

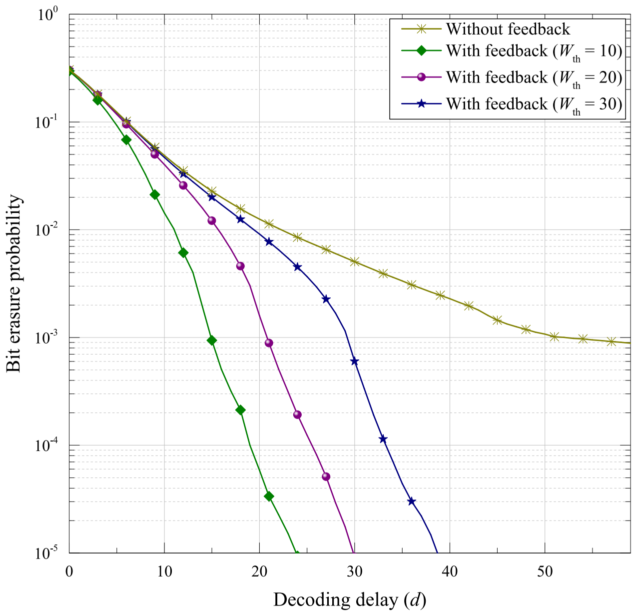

FIGURE 11. Impact of feedback window threshold on the average erasure probability performance.

request while varying the channel erasure probability (ϵ) and exponential rate parameter (λ). We observe that with the increment of ϵ and/or λ, the number of feedback request increases. Increasing ϵ reduces the error correction capability of the decoder, while increasing λ increases short cycles in the Tanner graph and hence, results in an increment of the feedback requests. Note that due to the retransmission, the proposed feedback scheme suffers from slight rate loss. The effective code rate after decoding time instant t is given by $R_{\text{eff}} = \frac{Kt}{Mt+N_f(t)}$. For the results shown in Fig. 9, the corresponding effective rates are provided in Fig. 10. In Fig. 11,

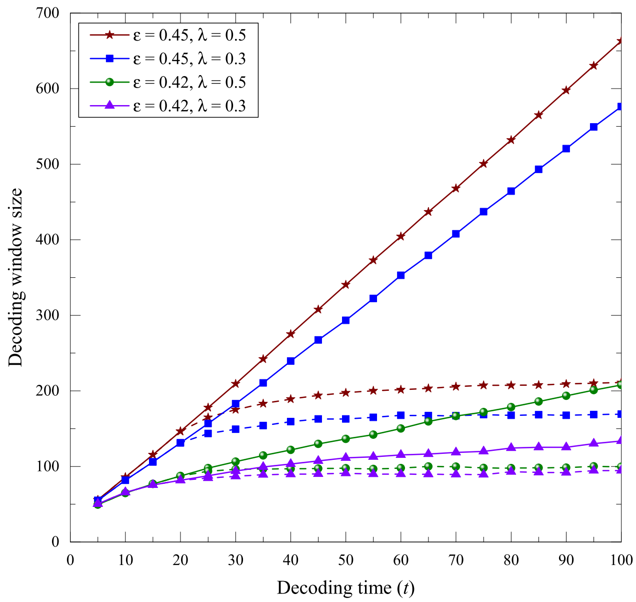

FIGURE 12. Decoding window size comparison with and without feedback. Solid lines present the scenario without feedback, while dotted lines represent the scenario with feedback.

we present the impact of the predefined threshold W_{th} on the erasure probability performance. We present the average erasure probability performance with respect to the decoding delay (d). As expected, the performance of the feedback strategy can be improved by decreasing W_{th}. However, a low W_{th} results in a large number of feedback requests. For example, with $W_{th} = 10, 20, 30$ the average number of retransmission requests required is 14.89, 1.75, 0.49, respectively at decoding time instant $t = 60$.

Recall that we consider peeling decoder [16] over the BEC. The proposed feedback strategy can be used along with the peeling decoder to further reduce the decoding complexity by reducing the size of the decoding window. For message size $M = 30$, Fig. 12 shows the decoding window size variation with respect to the decoding time instant while considering the scenarios with and without feedback. It is observed that the average decoding window size becomes a constant with the feedback strategy. In systems without feedback, the decoding window size grows with the decoding time instant due to the erasure floor observed in the performance. For both scenarios, we observe that the average decoding window size increases as the channel erasure probability and/or exponential parameter increases.

B. BIAWGN CHANNEL

Although the feedback strategy for the BEC is straightforward, this is not the case for BIAWGN channel. Unlike the BEC, the received bit over a BIAWGN channel cannot be declared as 1 or 0 with absolute certainty because of the presence of the Gaussian noise. Due to this uncertainty, a re-transmitted bit may cause degradation of the anytime performance instead of improving the performance. Thus retransmission of unreliable bits similar to the BEC is not appropriate for the BIAWGN channel. Note that, a feedback strategy for the BIAWGN channel was presented in [5] to improve the performance. However, a significant rate loss is observed due to the retransmission of the whole message in the feedback strategy of [5]. In this paper, we devise a novel feedback algorithm for the BIAWGN channel based on an adaptive parity check matrix.

At every time instant, the decoder searches for unreliable bits in the messages that have at least a decoding delay of W_{th}. We declare a code bit as reliable if the log-likelihood-ratio (LLR) output by the decoder for that bit is higher than $+L_{th}$ (for bit value 1) or lower than $-L_{th}$ (for bit value 0), where L_{th} is a predefined LLR threshold. Once unreliable bits are found, we activate the feedback link and instead of retransmission, we change the check matrix such that it ensures extra protection for the unreliable bit with the least index value. We refer to the unreliable bit with least index value as *tagged* bit. Once the feedback link is activated after time instant t, we modify the check matrix at both encoder and decoder in the following manner. We add E extra edges to the tagged bit node and connect those edges with E check nodes of position $t+1$. The modification in the Tanner graph due to the above feedback strategy is depicted in Fig. 13 with $E = 1$ and $M = 2$, where we assume that the index of the tagged bit is $i + 1$ after decoding time instant t. Thus, we add an extra edge (solid line in Fig. 13) to connect $(i + 1)^{th}$ information bit node and $(t + 1)^{th}$ check node. The procedure of the proposed feedback strategy is summarized in Algorithm 2. Unlike the feedback scheme for the BEC, the proposed feedback scheme for the BIAWGN channel does not lose any rate, since no extra bit retransmission is required for the proposed strategy. However the complexity of this feedback algorithm is higher than the feedback scheme for the BEC. This is due to the check matrix modification procedure performed in both encoder and decoder.

In Fig. 14, we present the numerical results regarding the performance improvement by using the above mentioned feedback strategy. In the simulation, we consider $(Q, A, \lambda, \gamma) = (4, 4, 0.2, 20)$ with SNR $= 0.5$ dB. For the feedback strategy, we set $E = 1$, $W_{th} = 20$ and $L_{th} = 10$. For three different messages, we observe performance improvements through the use of the feedback strategy. Note that a careful choice is required on selecting the value of E. Since a large value of E will introduce cycles in the Tanner graph, which may lead to performance degradation of the later messages. The decoder performs the BP decoding algorithm

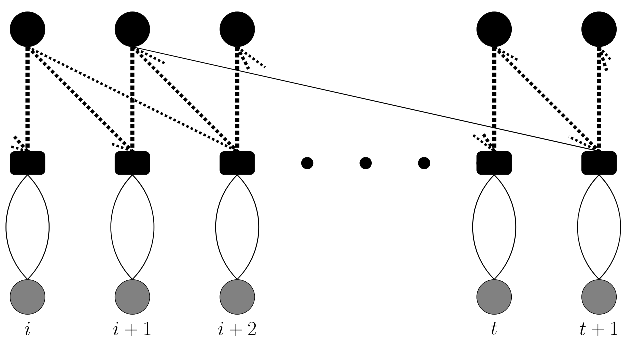

FIGURE 13. Modification in Tanner graph due to the proposed feedback strategy over the BIAWGN channel with $E = 1$ and $M = 2$ provided that the tagged bit (unreliable bit with least index) is the information bit of x_{i+1}. In the figure, the dotted lines with the information bit node represent the probabilistic edge connections, while the solid line with the information bit node represents the added deterministic edge.

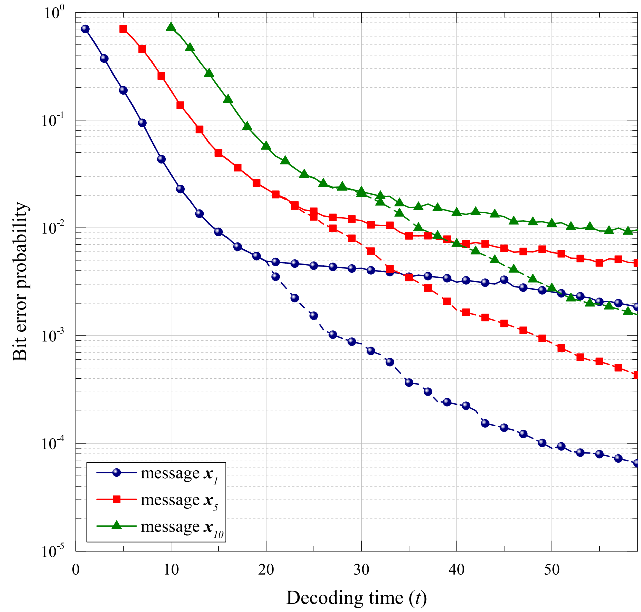

FIGURE 14. Impact of feedback window threshold on the performance of anytime codes.

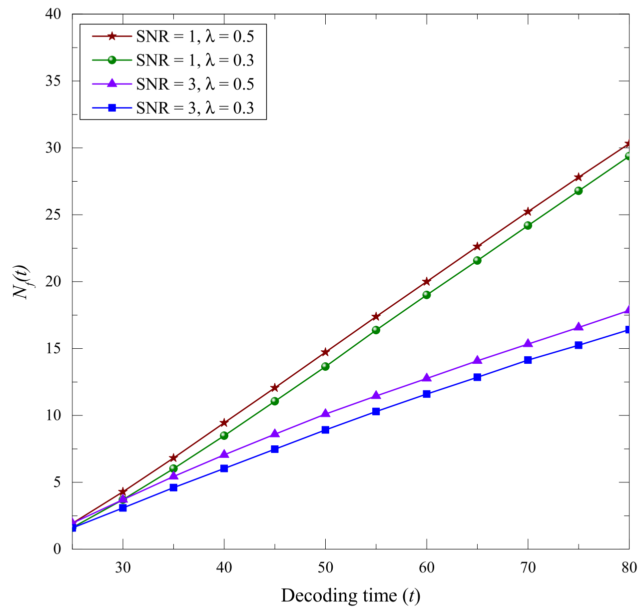

FIGURE 15. Impact of SNR and exponential rate parameter on the accumulated number of retransmission request $N_f(t)$.

(as described in Subsection II-C) by considering the added edge between the variable node that represents the tagged bit and the associated check node. In other words, the decoder performs the BP decoding by updating the entries of sets $\mathbb{S}_c(i)$ and $\mathbb{S}_v(j)$ (assume that the tagged bit is the i^{th} variable node and the associated check node is at j^{th} position). In Fig. 15, we show the accumulated number of retransmission request $N_f(t)$ required for this feedback strategy while varying the SNR and exponential rate parameter λ. We observe that for a given decoding time instant, $N_f(t)$ increases when SNR decreases and/or λ increases. Recall that, worsening the channel i.e., decreasing SNR reduces the error correction capability of the decoder, while increasing λ increases short cycles in the Tanner graph and hence, results in increment of the feedback requests. In Fig. 16, we compare our proposed feedback strategy with the feedback strategy of [5] and the feedback strategy with simple retransmission (similar to the scheme over BEC). It is observed that the feedback strategy of [5] provides better performance compared to our proposed scheme. However, note that a significant rate loss is observed for the feedback strategy of [5]. Specifically, at decoding time instant 50, the effective rate of the strategy of [5] is reduced from 0.5 to 0.452, while our proposed feedback strategy does not suffer from rate loss. On the other hand, the simple retransmission scheme exhibits worst performance (Retransmission 1 in the figure). We also plot the performance of the simple retransmission scheme when the tagged bit is retransmitted twice (Retransmission 2 in the figure). As expected, we observe a slight performance improvement for the later case, but it is still worse than our proposed feedback strategy. Furthermore, Retransmission 1 and Retransmission 2 suffer rate loss with effective rate of 0.493 and 0.485, respectively at decoding time instant 50.

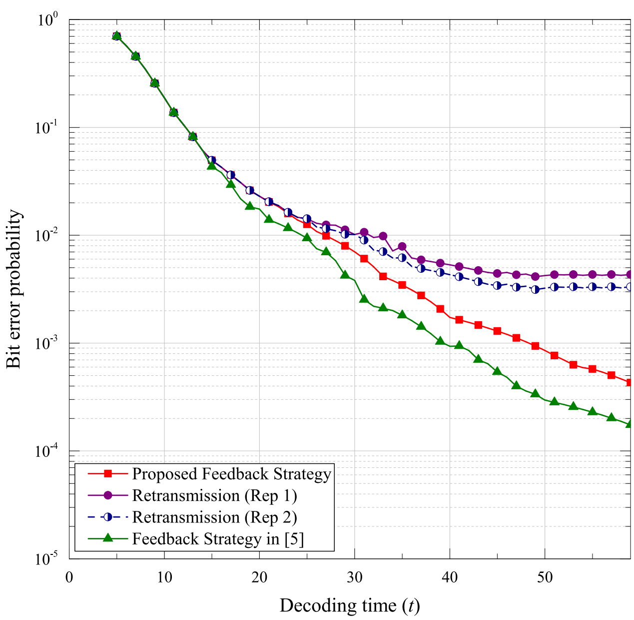

FIGURE 16. **Performance comparion between proposed and other feedback strategies.**

Algorithm 2 Anytime Transmission With Feedback for the BIAWGN Channel

- We set a thresholds W_{th} and L_{th}.
- When $t - W_{th} > 0$:
  - The anytime encoder does the following.
    - If the feedback link is not activated, the encoder generates $\boldsymbol{x}_{t+1}$ with the usual parity check matrix.
    - If the encoder receives a notification of an unreliable bit through the feedback link, it generates the message x_{t+1} based on a modified parity check matrix. Let the index of the tagged bit (unreliable bit with least index value) be j. To improve the reliability of the tagged bit, the Tanner graph of the parity check matrix is modified in the following manner. E extra edges are added with the variable node corresponding to the j^{th} coded bit and connect them with E check nodes at position $t+1$. With this modified parity check matrix, the encoder generates message $\boldsymbol{x}_{t+1}$ and sends it to decoder.
  - The anytime decoder does the following.
    - If the feedback is activated at previous time instant, the decoder modifies the check matrix in the similar manner as the encoder does and performs decoding operation on all received bits with modified check matrix.
    - Search for uncertain bits in the message from $\boldsymbol{x}_1(t)$ to $\boldsymbol{x}_{t-W_{th}}(t)$ based on the LLR threshold L_{th}.
    - If unreliable bits are observed, then it activates the feedback link and sends the index of the earliest unreliable bit through the feedback channel. Otherwise, the decoder stays silent.

Remarks: The feedback strategies proposed in this paper can be applied to other anytime codes including the codes proposed in [3]–[6]. However, the performance of the feedback strategy will vary depending on the code structure. For example, the feedback strategy over BIAWGN channel may not improve the performance of the anytime code proposed in [3]. This is due to the fact that the anytime code of [3] is highly dense, where the degrees of variable and check nodes increase linearly with the decoding time instant. Thus, addition of extra edges will result in more dense parity check matrix and may not improve the performance of the code.

V. IMPACT OF FEEDBACK TECHNIQUE IN CONTROL APPLICATIONS

We now demonstrate the impact of the feedback technique on tracking performance with a practical application. In general, an observable plant can be described by the following equations:

$$\dot{S} = AS + BU + \boldsymbol{n}_p \tag{16}$$

where $\boldsymbol{S}$ is the state of the system, $\boldsymbol{U}$ is the control input, $\boldsymbol{n}_p(t)$ is the process noise which are modeled as zero-mean additive white Gaussian noise with covariance matrix $\boldsymbol{Q}_p$. In this paper, we consider the tracking of an aircraft [19] with $\boldsymbol{S} = [w\ q\ \theta]$ and $\boldsymbol{U} = [\rho]$, where w is the vertical velocity, q is the pitch rate, θ is the pitch angle, and ρ is the elevator deflection angle. Following [19], $\boldsymbol{A}$ and $\boldsymbol{B}$ are specified by,

$$\boldsymbol{A} = \begin{bmatrix} -0.314 & -235.89 & 0 \\ -0.0034 & -0.428 & 0 \\ 0 & 1 & 0 \end{bmatrix}, \quad \boldsymbol{B} = \begin{bmatrix} -5.5\ 0.0021\ 0 \end{bmatrix}^T$$

For simplicity in the state estimation process, Eq. (16) can be discretised in the following form:

$$\boldsymbol{S}(k+1) = A_d\boldsymbol{S}(k) + B_d\boldsymbol{U}(k) + \boldsymbol{n}_p(k) \tag{17}$$

where $\boldsymbol{A}_d$ and $\boldsymbol{B}_d$ are obtained by performing the following operation on $\boldsymbol{A}$ and $\boldsymbol{B}$, respectively.

$$\boldsymbol{A}_d = \exp(\boldsymbol{A}\delta t) \simeq (\boldsymbol{I}) + \boldsymbol{A}\delta t$$
$$\boldsymbol{B}_d = \int_0^{\delta t} \exp(\boldsymbol{A}v)\boldsymbol{B}dv \simeq \boldsymbol{B}\delta t$$

where δt is the discretization step size. Different components of the state are usually measured by sensors embedded in the aircraft such as accelerometer, gyroscope, GPS sensors etc. Let $\boldsymbol{O}(k)$ be measured state by the sensors in the aircraft, which is defined by,

$$\boldsymbol{O}(k) = \boldsymbol{CS}(k) + \boldsymbol{n}_m(k),$$

where $\boldsymbol{C}$ is the measurement coefficient and $\boldsymbol{n}_m(k)$ is the measurement noise, which can be modeled as zero-mean additive white Gaussian noise with covariance matrix $\boldsymbol{Q}_m$. Then the measured state is quantized and mapped to K-bit message $\boldsymbol{m}_k \in \{0, 1\}^K$. We perform channel encoding on $\boldsymbol{m}_k$ such that we obtain an encoded message $\boldsymbol{x}_k \in \{0, 1\}^M$. In this paper, we consider three channel coding scenarios, where traditional block code was considered along with the anytime codes with and without feedback. After encoding, modulation is performed on $\boldsymbol{x}_k$ to transmit form the aircraft. We assume that the transmitter of the aircraft is connected with a remote receiver via a communication channel. Upon receiving the signal from the aircraft, the remote receiver subsequently performs demodulation, decoding, demapping, and state estimation. For the traditional block coding scheme, only the current state is estimated in each time step. On the other hand, current as well as previous states are estimated in each time step for the anytime coding scenarios. A generalised system model of the above described control problem is depited in Fig. 17. In this paper, we consider Kalman filter based estimation approach [20], [21], which can provide statistically optimum state estimation from the noisy version of observed data.

With the above setting, we now show the numerical results on the tracking performance while considering traditional block and anytime coding schemes. In the simulation, we consider $\boldsymbol{C} = [0\ 0\ 1]$ and hence only pitch angle was measured. A 16-bit uniform quantization was performed on the measured pitch angle, and the channel was modeled as erasure

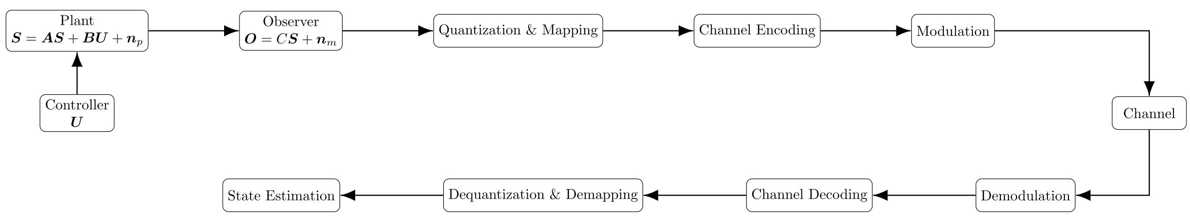

FIGURE 17. Overall system for the control problem.

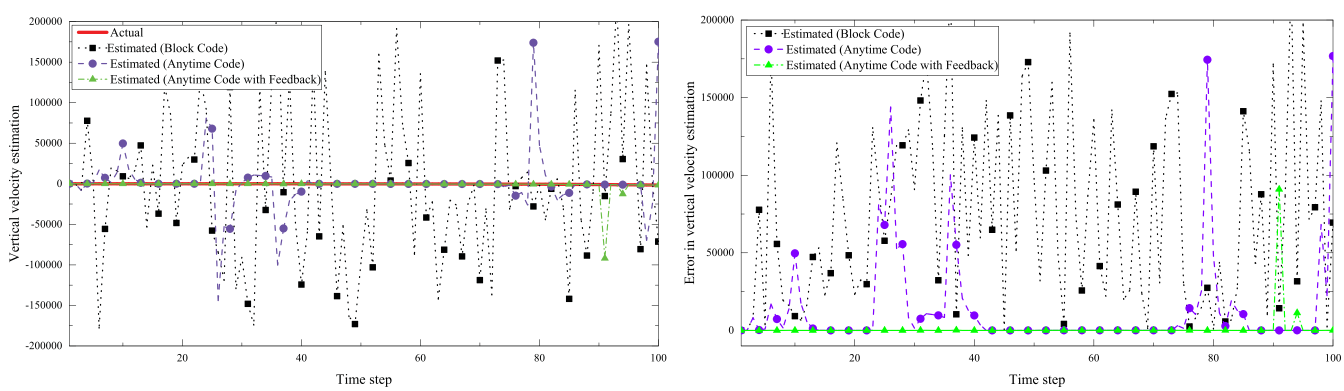

(a) (b)

FIGURE 18. Vertical velocity estimation and error performance comparison. (a) Estimation performance. (b) Error performance.

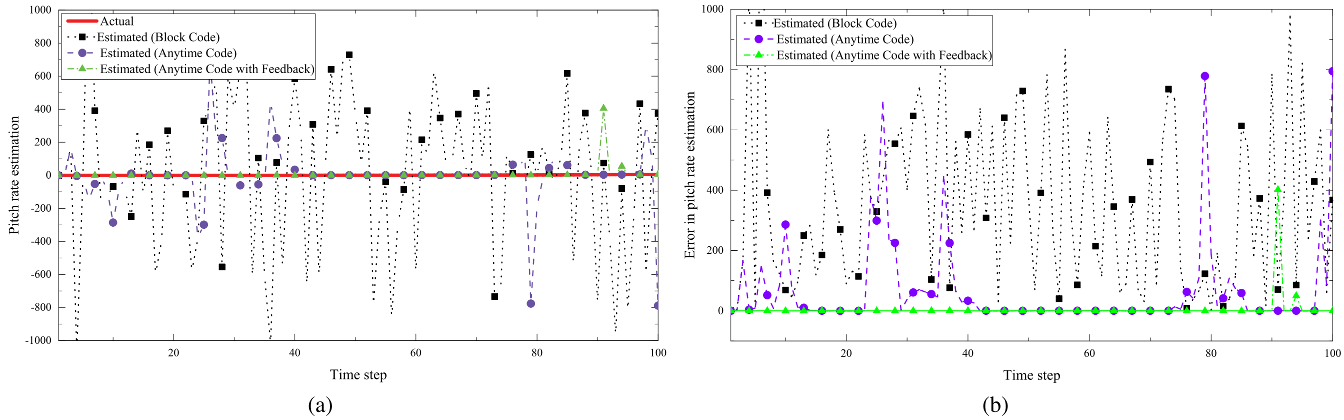

FIGURE 19. Pitch rate estimation and error performance comparison. (a) Estimation performance. (b) Error performance.

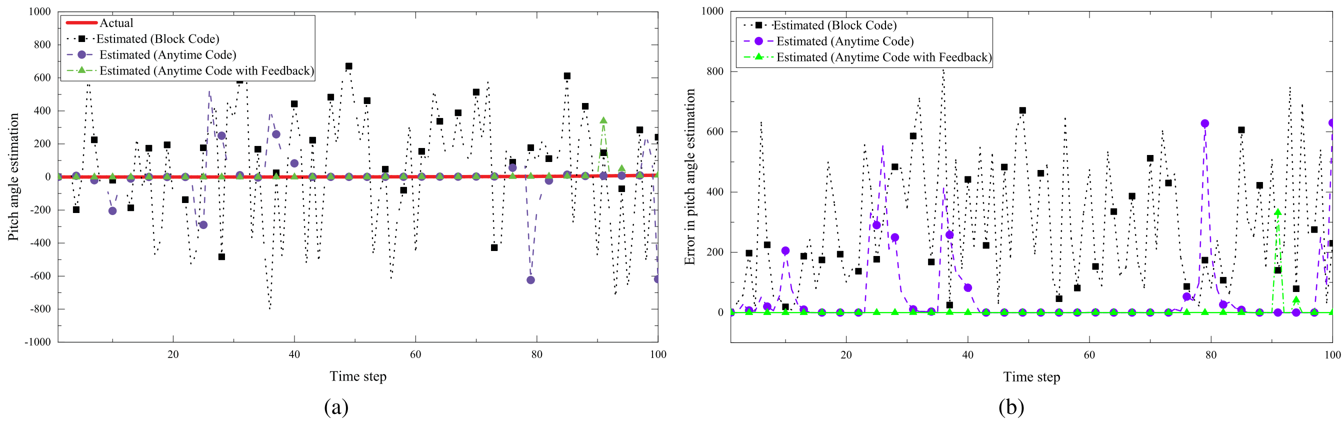

FIGURE 20. Pitch angle estimation and error performance comparison. (a) Estimation performance. (b) Error performance.

channel with $\epsilon = 0.44$. For the anytime code, we consider a $(Q, A, \lambda, \gamma) = (4, 4, 0.1, 10)$-SC-RA code and set $W_{th} = 5$ for the feedback strategy. For the block code, we consider a $(Q, A) = (4, 4)$-RA block code. The tracking performance, presented in the simulation results, is realized for a period of 15s, where 150 steps are considered with step size $\delta t = 0.1$s. The process and measurement noise co-variances are set as $\boldsymbol{Q}_p = \boldsymbol{Q}_m = 0.0025\boldsymbol{I}$, with the input (elevator deflection angle) $\rho = 0.2$ rad. In Fig. 18 to Fig. 20, we present the state estimation performance while considering the estimation of velocity, pitch rate, and pitch angle, respectively. Results are presented for block and anytime coding schemes. It is observed that the block code exhibits worse performance compared to the anytime coding schemes. Among the performance of anytime codes, we observe that the deviation of the estimated state from the actual state is less with the feedback strategy compared to the scenario without feedback. Along with the estimation results, corresponding absolute error results are also presented in Fig. 18 to Fig. 20, where nearly zero error was observed with the proposed anytime coding with feedback technique.

VI. CONCLUSION

In this paper, we have shown the design of low complexity anytime codes constructed from spatially coupled RA codes. An asymptotic analysis of the proposed anytime code is presented over two different channels (BEC and BIAWGN channel) and it is shown that the proposed SC-RA anytime codes outperform its counterpart SC-LDPC anytime codes. Extensive numerical results are presented while varying code and channel parameters. From the results, we have observed that anytime SC-RA codes are not able to maintain their desired anytime characteristics and end up with erasure/error floor, however, the code design needs to satisfy practical demands like finite-length memory and/or high delay-exponent. To eliminate the high erasure floor for such scenarios, a retransmission based feedback strategy is presented for the BEC. We have shown that the erasure floor in the anytime performance can be avoided at a large extent using proposed feedback strategies, in which only few feedback requests need to be made. Moreover, it is shown that the anytime decoding complexity can be reduced with feedback strategy. Since the retransmission scheme is not suitable for BIAWGN channels, we have devised a novel feedback strategy based on an adaptive parity check matrix for BIAWGN channels. Similar to the BEC, a performance improvement through the proposed feedback strategy is observed over BIAWGN channels. However, the feedback strategy for BIAWGN posses higher complexity than the feedback strategy shown for the BEC. We have also demonstrated the effectiveness of the proposed strategy by applying it to an aircraft tracking application.

REFERENCES

[1] A. Sahai and S. Mitter, "The necessity and sufficiency of anytime capacity for stabilization of a linear system over a noisy communication link—Part I: Scalar systems," *IEEE Trans. Inf. Theory*, vol. 52, no. 8, pp. 3369–3395, Aug. 2006.
[2] A. Sahai, "Anytime information theory," Ph.D. dissertation, Dept. Elect. Eng. Comput. Sci., Massachusetts Inst. Technol., Cambridge, MA, USA, 2001.
[3] L. Grosjean, "Practical anytime codes," Ph.D. dissertation, KTH Roy. Inst. Technol., Stockholm, Sweden, 2016.
[4] A. Tarable, A. Nordio, F. Dabbene, and R. Tempo, "Anytime reliable LDPC convolutional codes for networked control over wireless channel," in *Proc. IEEE Int. Symp. Inf. Theory (ISIT)*, Jul. 2013, pp. 2064–2068.
[5] N. Zhang, M. Noor-A-Rahim, B. N. Vellambi, and K. D. Nguyen, "Anytime characteristics of protograph-based LDPC convolutional codes," *IEEE Trans. Commun.*, vol. 64, no. 10, pp. 4057–4069, Oct. 2016.
[6] M. Noor-A-Rahim, K. D. Nguyen, and G. Lechner, "Anytime reliability of spatially coupled codes," *IEEE Trans. Commun.*, vol. 63, no. 4, pp. 1069–1080, Apr. 2015.
[7] M. Noor-A-Rahim, K. D. Nguyen, and G. Lechner, "Anytime spatially coupled codes for relay channel," in *Proc. Austral. Commun. Theory Workshop (AusCTW)*, Feb. 2014, pp. 39–44.
[8] A. Sahai, "Why do block length and delay behave differently if feedback is present?" *IEEE Trans. Inf. Theory*, vol. 54, no. 5, pp. 1860–1886, May 2008.
[9] A. Sahai, S. Avestimehr, and P. Minero, "Anytime communication over the Gilbert–Eliot channel with noiseless feedback," in *Proc. Int. Symp. Inf. Theory (ISIT)*, Sep. 2005, pp. 1783–1787.
[10] P. Minero and M. Franceschetti, "Anytime capacity of Markov channels," in *Proc. IEEE Int. Symp. Inf. Theory (ISIT)*, Jun. 2015, pp. 61–65.
[11] A. Sahai and Q. Xu, "The anytime reliability of the AWGN+erasure channel with feedback," in *Proc. 43rd Annu. Allerton Conf. Commun., Control, Comput.*, Sep. 2004, pp. 1250–1276.
[12] H. T. Simsek, "Anytime channel coding with feedback," Ph.D. dissertation, Dept. Eng. Elect. Eng. Comput. Sci., Univ. California, Berkeley, Berkeley, CA, USA, 2004.
[13] S. Kudekar, T. J. Richardson, and R. L. Urbanke, "Threshold saturation via spatial coupling: Why convolutional LDPC ensembles perform so well over the BEC," *IEEE Trans. Inf. Theory*, vol. 57, no. 2, pp. 803–834, Feb. 2011.
[14] S. Johnson and G. Lechner, "Spatially coupled repeat-accumulate codes," *IEEE Commun. Lett.*, vol. 17, no. 2, pp. 373–376, Feb. 2013.
[15] J. Thorpe, "Low-density parity-check (LDPC) codes constructed from protographs," JPL IPN Prog. Rep. 42–154, 2003.
[16] M. G. Luby, M. Mitzenmacher, M. A. Shokrollahi, D. A. Spielman, and V. Stemann, "Practical loss-resilient codes," in *Proc. ACM Symp. Theory Comput.*, 1997, pp. 150–159, doi: 10.1145/258533.258573.
[17] S. J. Johnson, *Iterative Error Correction: Turbo, Low-Density Parity-Check and Repeat-Accumulate Codes*. Cambridge, U.K.: Cambridge Univ. Press, Jan. 2010.
[18] M. Noor-A-Rahim, G. Lechner, and K. D. Nguyen, "Density evolution analysis of spatially coupled LDPC codes over BIAWGN channel," in *Proc. Austral. Commun. Theory Workshop (AusCTW)*, Jan. 2016, pp. 13–17.
[19] L. Chrif and Z. M. Kadda, "Aircraft control system using LQG and LQR controller with optimal estimation-Kalman filter design," *Procedia Eng.*, vol. 80, pp. 245–257, 2014. [Online]. Available: http://www.sciencedirect.com/science/article/pii/S1877705814011771
[20] B. D. O. Anderson and J. B. Moore, *Optimal Filtering*. Englewood Cliffs, NJ, USA: Prentice-Hall, 1979.
[21] R. Olfati-Saber, "Distributed Kalman filtering for sensor networks," in *Proc. IEEE Conf. Decis. Control*, Dec. 2007, pp. 5492–5498.

MD. NOOR-A-RAHIM received the Ph.D. degree in telecommunications from the Institute for Telecommunications Research, University of South Australia, Australia, in 2015. He is currently a Research Fellow with the Centre for Infocomm Technology, Nanyang Technological University, Singapore. His research interests include information theory, wireless communications, and vehicular communications. He is a recipient of the Michael Miller Medal for the most outstanding Ph.D. thesis from the School of Information Technology & Mathematical Sciences, University of South Australia, in 2015.

M. O. KHYAM received the Ph.D. degree in electrical engineering from The University of New South Wales, Australia, in 2015. From 2016 to 2017, he was a Post-Doctoral Research Fellow with the National University of Singapore. He was also a Post-Doctoral Research Fellow with the Nanyang Technological University, Singapore, from 2017 to 2018. He is currently a Post-Doctoral Research Fellow with the Virginia Tech, USA. His research interests include signal processing and wireless communication.

YONG LIANG GUAN is currently a Tenured Associate Professor with the School of Electrical and Electronic Engineering, Nanyang Technological University, Singapore. He has led 13 past and present externally funded research projects on advanced wireless communication techniques, coding for 10Terabits-per-square-inch magnetic recording, acoustic telemetry for drilling application etc. with total funding of over SGD 9 million. He has published an invited monograph, three book chapters, and over 300 journal and conference papers. His research interests broadly include coding, signal design and signal processing for communication systems, storage systems, and information security systems. He is an Associate Editor of the IEEE Transactions on Vehicular Technology, the Chair of the IEEE ComSoc Singapore Chapter, and the AE of the IEEE Signal Processing Letter.

G. G. MD. NAWAZ ALI received the B.Sc. degree from the Khulna University of Engineering & Technology, Bangladesh, in 2006, and the Ph.D. degree from the Department of Computer Science, City University of Hong Kong, in 2013. After graduation, he was a Researcher with the Department of Computer Science, City University of Hong Kong, for a while. Then, he joined as an Assistant Professor at the Department of Computer Science and Engineering, Khulna University of Engineering & Technology. Since 2015, he was a Post-Doctoral Research Fellow with the School of Electrical and Electronic Engineering, Nanyang Technological University, Singapore. He is currently a Post-Doctoral Research Fellow with the Department of Automotive Engineering, Clemson University, USA. His current research interests include network coding, wireless broadcasting, mobile computing, and ad hoc networking. He is a member of the IEEE VTS. He is a reviewer of a number of international journals including the IEEE Transactions on Intelligent Transportation Systems and Magazine, the IEEE Transactions on Vehicular Technology, and the *Wireless Networks*.

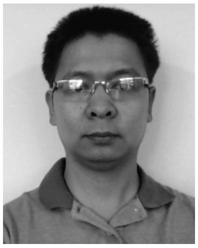

KHOA D. NGUYEN received the B.Eng. degree in electrical and electronics engineering from The University of Melbourne in 2005, and the Ph.D. degree in telecommunications from the Institute for Telecommunications Research, University of South Australia in 2010. He is currently a Senior Research Fellow with the Institute for Telecommunications Research, University of South Australia. His research interests include adaptive communications, delay-limited communications, coding theory, and information theory.

GOTTFRIED LECHNER received the Dipl.-Ing. and Dr.techn. degrees from the Vienna University of Technology, Vienna, Austria, in 2003 and 2007, respectively. From 2002 to 2008, he was a Researcher in the area of signal and information processing at the Telecommunications Research Centre Vienna (ftw). He is currently an Associate Research Professor and the Director of the Institute for Telecommunications Research, University of South Australia, Adelaide, Australia. His research interests include sparse graph codes, iterative techniques, and wireless communications with a focus on satellite communications. He is a member of the IEEE Information Theory and Communications Societies.